

Mitochondrial Transfer Induced by Adipose-Derived Mesenchymal Stem Cell Transplantation Improves Cardiac Function in Rat Models of Ischemic Cardiomyopathy

Cell Transplantation
Volume 32: 1–12
© The Author(s) 2023
Article reuse guidelines:
sagepub.com/journals-permissions
DOI: 10.1177/09636897221148457
journals.sagepub.com/home/cll


Daisuke Mori¹ , Shigeru Miyagawa¹, Takuji Kawamura¹, Daisuke Yoshioka¹, Hiroki Hata¹, Takayoshi Ueno¹, Koichi Toda¹, Toru Kuratani¹, Miwa Oota^{2,3}, Kotoe Kawai^{2,3}, Hayato Kurata^{2,3}, Hiroyuki Nishida^{2,3}, Akima Harada¹, Toshihiko Toyofuku⁴, and Yoshiki Sawa^{1,5}

Abstract

Although mesenchymal stem cell transplantation has been successful in the treatment of ischemic cardiomyopathy, the underlying mechanisms remain unclear. Herein, we investigated whether mitochondrial transfer could explain the success of cell therapy in ischemic cardiomyopathy. Mitochondrial transfer in co-cultures of human adipose-derived mesenchymal stem cells and rat cardiomyocytes maintained under hypoxic conditions was examined. Functional recovery was monitored in a rat model of myocardial infarction following human adipose-derived mesenchymal stem cell transplantation. We observed mitochondrial transfer *in vitro*, which required the formation of cell-to-cell contacts and synergistically enhanced energy metabolism. Rat cardiomyocytes exhibited mitochondrial transfer 3 days following human adipose-derived mesenchymal stem cell transplantation to the ischemic heart surface post-myocardial infarction. We detected donor mitochondrial DNA in the recipient myocardium concomitant with a significant improvement in cardiac function. Mitochondrial transfer is vital for successful cell transplantation therapies and improves treatment outcomes in ischemic cardiomyopathy.

Keywords

adipose derived mesenchymal stem cell, mitochondrial transfer, ischemic cardiomyopathy, gap junction, epicardial cell transplantation

Introduction

Ischemic heart disease is a leading cause of death worldwide. Various cell therapies have been applied to treat acute myocardial infarction (MI) and ischemic cardiomyopathy. However, the mechanisms underlying these responses remain to be fully elucidated^{1–3}. Recently, a phenomenon called mitochondrial transfer (MT) via nanotube has been described in animal models of acute lung injury following mesenchymal stem cell (MSC) transplantation. MT is thought to exert protective effects on recipient alveolar epithelial cells, thereby representing an uninvestigated mode of action of cell therapy against heart failure^{4–6}. MT is carried out through a structure called gap junction, which is a part where cells are close to each other, and a structure in which intercellular communication is formed by a protein called connexin that penetrates the cell membrane. Bidirectional MT has been observed in cardiomyocytes (CMs) co-cultured

with MSCs^{4,7}. CMs receiving mitochondria show elevated expression of mitochondrial proteins, increased oxidative phosphorylation, and improved ATP production⁸. *In vivo*,

¹ Department of Cardiovascular Surgery, Osaka University Graduate School of Medicine, Suita, Japan

² Institute of Advanced Stem Cell Therapy, Osaka University, Osaka, Japan

³ ROHTO Pharmaceutical Co., Ltd., Osaka, Japan

⁴ Institute of Immunology and Regenerative Medicine, Osaka University, Osaka, Japan

⁵ Medical Centre for Translational and Clinical Research, Osaka University Hospital, Osaka, Japan

Submitted: May 21, 2022. Revised: August 24, 2022. Accepted: December 13, 2022.

Corresponding Author:

Yoshiki Sawa, Department of Cardiovascular Surgery, Osaka University Graduate School of Medicine, Suita 565-0871, Japan.
Email: sawa-p@surg1.med.osaka-u.ac.jp



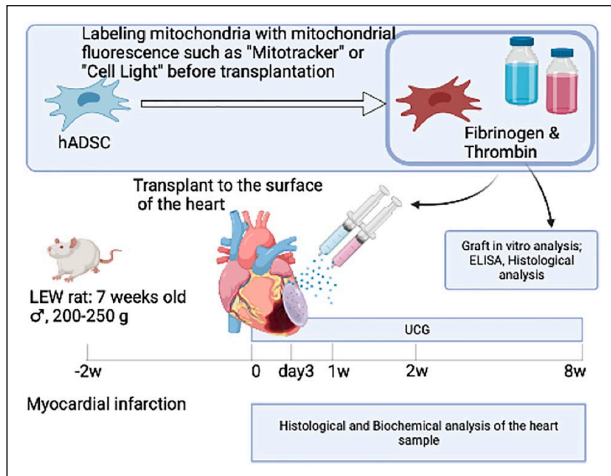


Figure 1. Study protocol. Myocardial infarction was induced in 7- to 8-week-old male rats 2 weeks prior to transplantation. During transplantation, human adipose-derived stem cells (hADSCs) with or without pre-stained mitochondria were implanted using fibrin glue on the surface of the heart. Following transplantation, heart samples were obtained at scheduled time points for various analyses and cardiac function was evaluated using echocardiography. The hADSC grafts were analyzed *in vitro*.

MT is expected to confer resistance to cytotoxicity, exert anti-apoptotic effects, and increase ATP production in recipient CMs, overall improving myocardial function^{9,10}.

To the best of our knowledge, it has not been evaluated previously whether MT occurs *in vivo* following cell transplantation. Hence, the role of MT in the success of cell transplantation and its effect on heart function remain unknown. Here, we demonstrated MT from transplanted cells to CMs *in vivo* and proposed that this phenomenon represents the mechanism underlying successful cell therapies for ischemic cardiomyopathy.

Materials and Methods

Assessment of *In Vivo* MT

Transplantation of human adipose-derived stem cells (hADSCs) harboring stained mitochondria. Experimental protocols were approved by the Ethics Review Committee for Animal Experimentation of Osaka University Graduate School of Medicine (Reference number 02-030-002), Japan. Animal care was conducted humanely, in compliance with the Principles of Laboratory Animal Care formulated by the National Society for Medical Research and the Guide for the Care and Use of Laboratory Animals prepared by the Institute of Animal Resources and published by the National Institutes of Health (Eighth Edition, revised 2011).

A MI model in F344/NJcl-rnu/rnu rats (CLEA Japan, Inc., Tokyo, Japan) was generated via permanent ligation of the left anterior descending artery (LAD). Two weeks after

LAD ligation, hADSCs (1×10^6 cells; Lonza, Tokyo, Japan) were transplanted into the infarct area using fibrinogen and thrombin solution (CSL Behring, Tokyo, Japan). The composition of this graft is shown in S1 Table¹¹. The hADSCs were pre-stained with MitoTracker Red (Thermo Fisher Scientific, Waltham, MA, USA)¹². The rats were euthanized at appropriate time points following transplantation, and heart samples were collected (Fig. 1). Subcutaneous injection of caprophen and inhaled isoflurane were used to relieve the pain of the animals, and at the time of euthanasia, overdose of inhaled isoflurane and intravenous potassium chloride were administered to obtain cardiac arrest. Following formalin fixation, paraffin-embedded heart sections were stained with an antibody against phalloidin (Cat. #A12379; Thermo Fisher Scientific), and counterstained with Hoechst 33342 (Dojindo Molecular Technologies, Inc., Kumamoto, Japan).

Observation of graft-heart boundaries with electron microscopy. Mitochondrial ultrastructure and spatial relationship between hADSCs and rat cardiomyocytes (rCMs) were assessed in tissue samples collected from areas including the boundary between the heart and hADSC graft. Contrasted sections were imaged under an H-7500 transmission electron microscope (Hitachi, Tokyo, Japan) (Fig. 2A–G).

Detection of donor mitochondrial DNA in recipient rCMs. Paraffin-embedded tissues from the heart and hADSC grafts were harvested 3 days after transplantation. Tissue sections were stained with hematoxylin and eosin, and residual rCMs around the fibrotic tissue and just beneath the hADSC graft were collected using a laser-equipped microscope (Leica LMD7000). DNA was isolated, and a human mitochondrial DNA fragment was amplified using a customized primer pair (Eurofins Genomics, Louisville, KY, USA) (Fig. 2H–J) (S2 Table)^{13–15}. PCR conditions and reaction mixtures are listed in S3 and S4 Tables. The PCR products were purified and used as a template for sequencing and further analysis.

Intravital imaging of MT from hADSC grafts to the beating myocardium. MI-induced adult male CAG/eGFP transgenic Sprague–Dawley (SD) rats (200–250 g; Japan SLC, Inc., Shizuoka, Japan) were used as recipients of hADSC transplants. The hADSCs were transfected using CellLight™ Mitochondria-RFP BacMam 2.0 (Thermo Fisher Scientific) (Fig. 3A). Graft composition and transplantation were performed as above (S1 Table). The beating heart and the graft were stabilized using a custom-made suction device (Fig. 3B)¹⁶. Clear *in vivo* images were obtained by previously reported methods¹⁷. Observation was initiated immediately following transplantation and continued for the maximum possible duration.

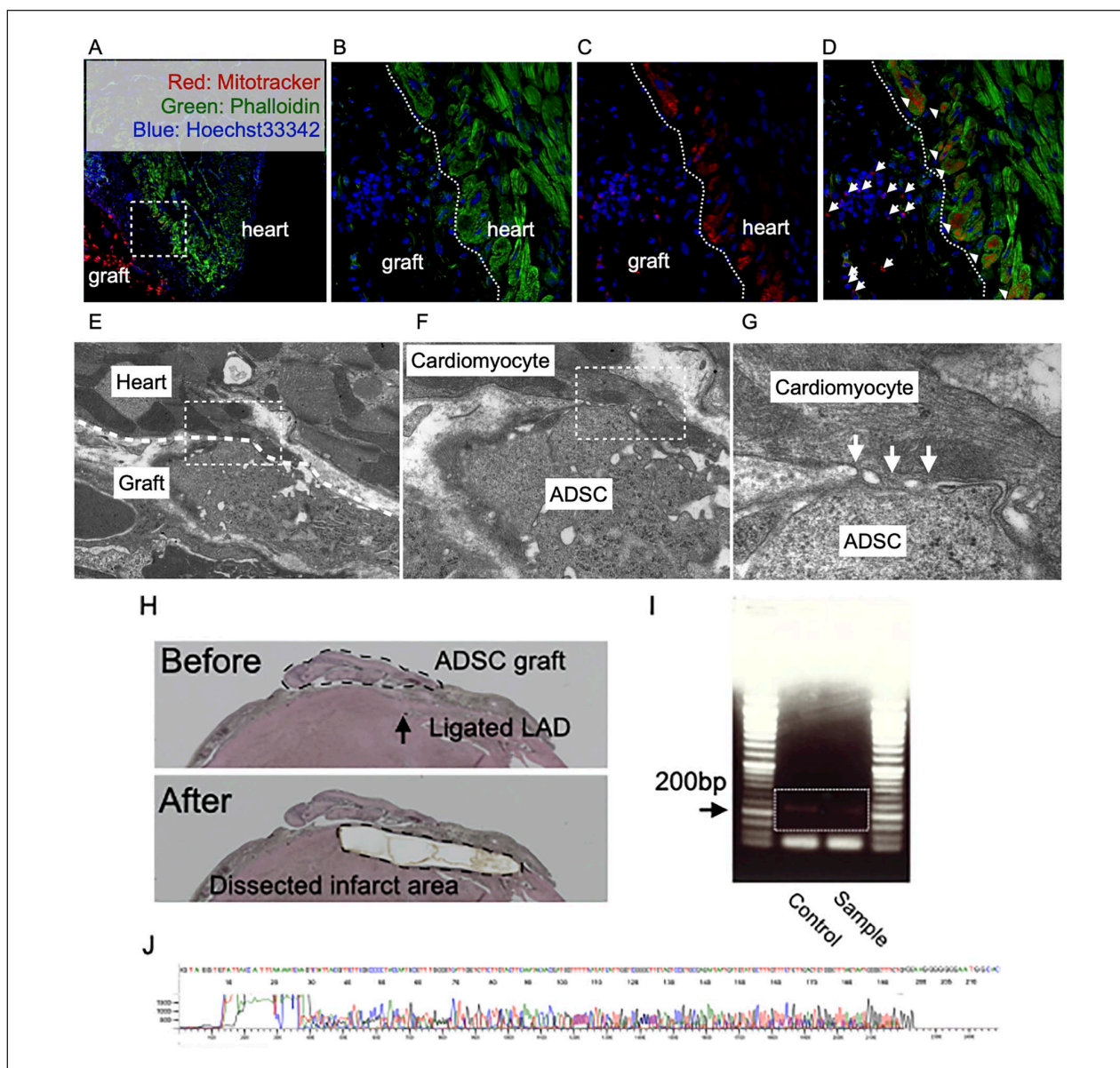


Figure 2. Evaluation of mitochondrial transfer (MT) *in vivo*. (A) Three days following transplantation, hADSC graft-derived mitochondria were observed in recipient rCMs; the mitochondria under epicardium and in the hADSC graft were also stained. This transfer phenomenon was observed only in rats with myocardial infarction (MI). (B, C) Individual staining for rat actin and human mitochondria are shown in the dashed line box in A. (D) Magnified picture of the dashed line box in A. Arrow: mitochondria in hADSC; arrowhead: mitochondria in rat CM; red: mitochondria of ADSC; green: actin in rCM; blue: nucleus. (E) Electron microscopy image of the graft and heart boundary. (F) Magnified picture of the dashed rectangle in E. (G) Magnified picture of the dashed rectangle in F. Arrows indicate pseudopod-like structures or fusion. (H) Heart sample used for sequencing of the donor mitochondrial DNA fragment. The samples for sequencing were micro-dissected and obtained from the part enclosed by a dashed line. (I) Before and after cutting out the gel containing target amplicons (rectangle), of approximately 200–250 bp, following electrophoresis. (J) Gene sequence homology to human MT-ND6. MT-ND6: mitochondrially encoded NADH-ubiquinone oxidoreductase core subunit 6; CM: cardiomyocyte; ADSC: adipose-derived stem cell; rCM: rat cardiomyocyte.

In Vitro Observation of MT and Its Influence on rCM Metabolism

Observation of rCM and hADSC co-culture. Commercially available neonatal rCMs (RCM-561; QBM Cell Science,

Ontario, Canada) were stained with MitoTracker Green (Thermo Fisher Scientific), seeded on a 4-well glass slide chamber, and cultured under normoxic conditions for 3–4 h. The same count of hADSCs, stained with MitoTracker Red (Thermo Fisher Scientific), was transferred to the rCM

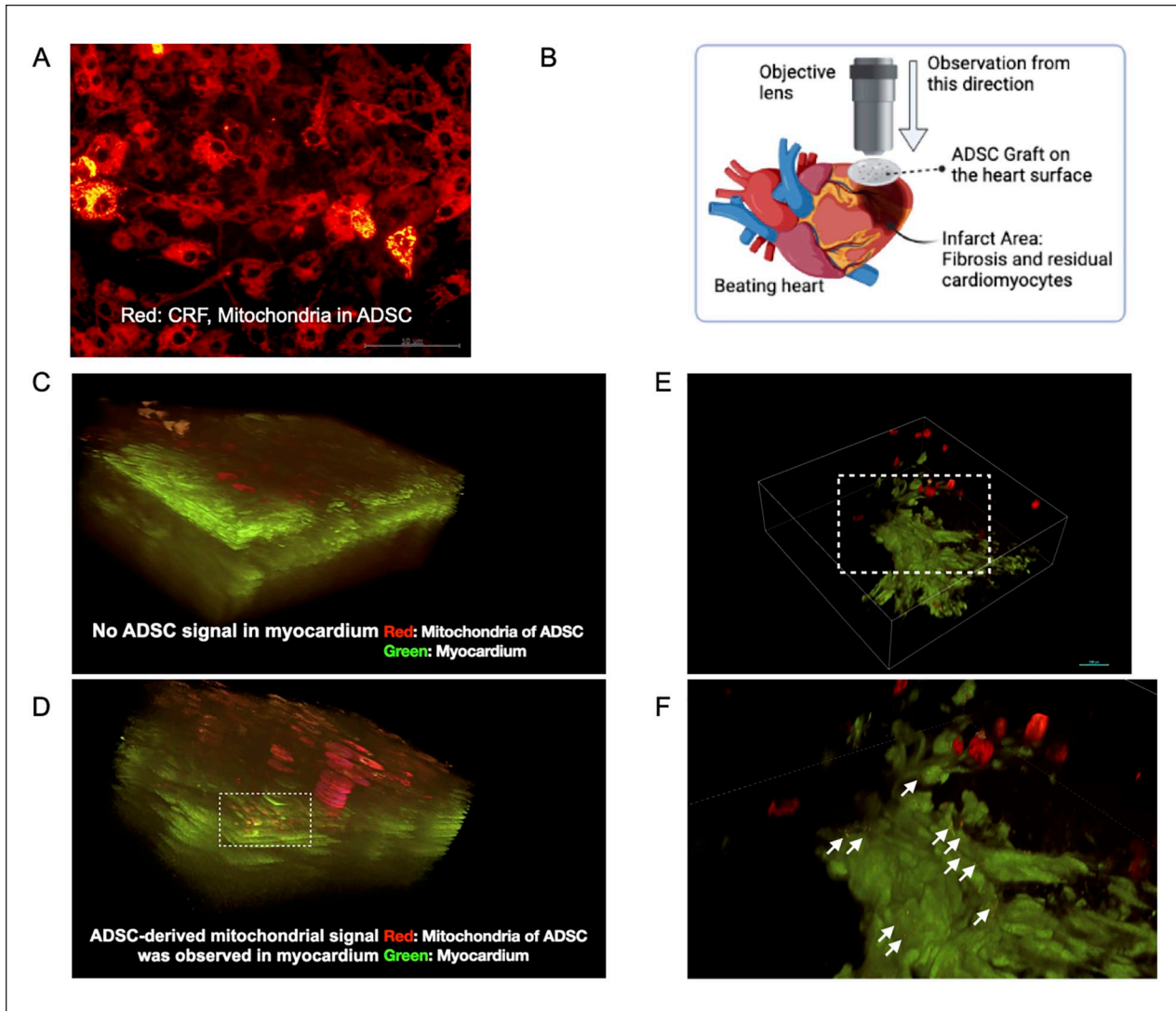


Figure 3. Intravital imaging of mitochondrial transfer (MT). (A) hADSCs transfected with CellLight to express RFP in the mitochondria. (B) Schematic illustration of intravital imaging. The residual rCMs in the infarct area were observed through the stabilizer and graft. (C) Spatial relationship between the graft and heart at the beginning of observation. (D) RFP signal in the rCMs just beneath the pericardium (rectangle) 6 h after grafting. (E) Representative image of residual rCMs in the infarct area. Arrows indicate transferred granular mitochondria. (F) Magnified picture of the dashed rectangle in E. hADSC: human adipose-derived stem cell; rCM: rat cardiomyocyte; RFP: red fluorescent protein.

culture, and the two cell populations were co-cultured for 1 h before observation (Fig. 4A) under hypoxic conditions (1% O₂), with or without 10 μM α-glycyrrhethinic acid (αGA; Sigma-Aldrich, St. Louis, MO, USA), for 24 h. Subsequently, co-cultured cells were fixed and stained with anti-cardiac actinin and anti-human mitochondria antibodies, and three-dimensional images were constructed.

Measurement of oxygen consumption rate (OCR). OCR in living cells was measured using a Seahorse XF24 Extracellular Flux Analyzer (Agilent Technologies, Santa Clara, CA, USA), according to the manufacturer's protocol. The rCMs (2 × 10⁴ cells/well) were cultured on 96-well Agilent Seahorse

XF cell culture microplates under normoxic conditions for 48 h, after which the same number of hADSCs were added to each well and cultured with or without αGA, under normoxic conditions, for 24 h before analysis. The detailed culture conditions for each group are listed in S5 Table¹⁸.

Quantification of cytokines from the hADSC graft. hADSC grafts were cultured under normoxic or hypoxic (1% O₂) conditions, and culture supernatant was collected after 24, 48, and 72 h. The secretion of hepatocyte growth factor (HGF), vascular endothelial growth factor (VEGF), IL-6, and IL-10 was assessed by enzyme-linked immunosorbent assays (R&D Systems, Minneapolis, MN, USA).

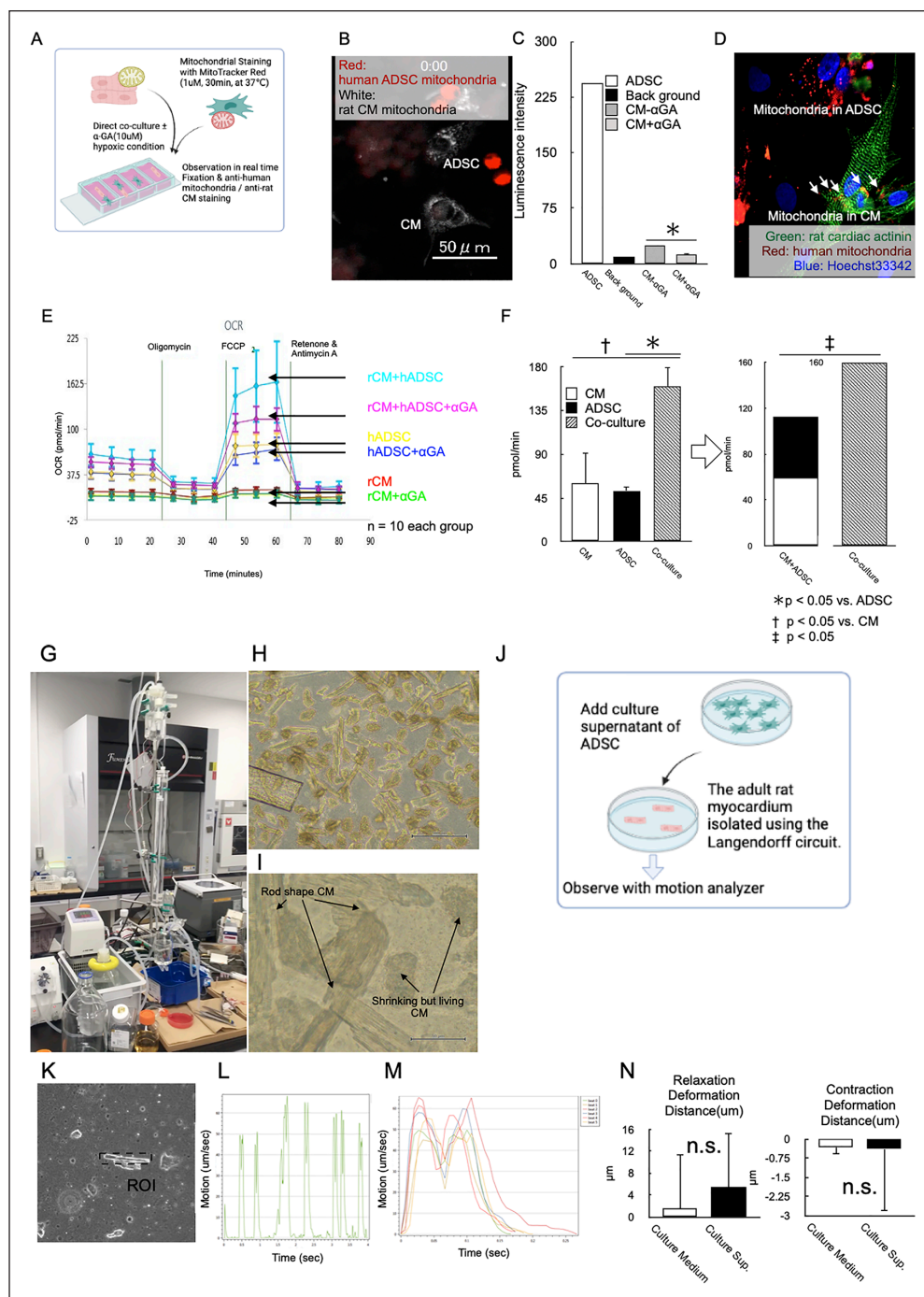


Figure 4. Co-culture of rCMs and hADSCs. (A) This is the protocol for this experiment. rCMs were cultured on chamber slides under normoxic conditions for 3–4 h, and pre-stained hADSCs were added thereafter. After starting the co-culture, the chamber slides were observed in real time. After observation, the cells were fixed and stained with anti-human mitochondria and anti-rat mitochondria antibodies. (B) Real-time continuous observations over 24 h with or without α GA. (C) Mitochondrial luminescence intensity in rCMs and culture medium. (D) Fixed co-culture samples showing the transferred granular mitochondria in rCMs; $n = 4$ samples per group. * $P < 0.05$ by t -test. (E, F) Effect of α GA on OCR of rCMs and hADSCs cultured independently or co-cultured; $n = 10$ per group. * $P < 0.05$, † $P < 0.05$, ‡ $P < 0.05$ by ANOVA. (G) Illustration of the isolation system of adult rCMs. (H, I) Representative image of harvested rCMs. (J) Sequence of this experiment: culture supernatant of hADSCs was collected and added to the freshly isolated adult rCMs for motion analysis. (K) In motion analysis, the region of interest was set independently for each adult rCM. (L, M) Representative velocity waveforms. (N) Effect of hADSC culture supernatant on rCM contractions. hADSC: human adipose-derived stem cell; rCM: rat cardiomyocyte; OCR: oxygen consumption rate; α GA: α -glycyrrhetic acid.

Isolation and motion analysis of rCMs with/without hADSC supernatant. The 7- to 8-week-old male Crl: (SD) rats were generally anesthetized, and the hearts were harvested. The heart was connected to a Langendorff circulation circuit through aortic ligation to the cannula (Fig. 4G). Perfusion buffer (Tyrode's solution, S6 Table) containing 300 units/mL collagenase type II (Gibco; Thermo Fisher Scientific) was perfused into the coronary arteries. The heart was homogenized on a petri dish, and cardiac cells were transferred to a 96-well plate (Fig. 4H, I). The rCMs were stimulated with either 1 μ M isoprenaline, 400 μ M propranolol, or hADSC culture supernatant (Fig. 4J). rCM motion was observed and analyzed using the SI8000 Cell Motion Imaging System (Sony, Tokyo, Japan)^{19,20}.

Evaluation of Influence of MT on Cardiac Function and Metabolism

Graft survival following transplantation. Luciferase-transduced hADSCs were transplanted into the nude rat MI model as described above (Fig. 5A). The luminescence intensity of the grafts was measured at the body surface. For histological analysis, hearts with residual graft samples were collected at days 1, 3, 7, and 14, and paraffin-embedded samples were stained using an antibody specific to human mitochondria (Cat. #MAB1273; Merck Millipore, Burlington, MA, USA).

Assessment of cardiac function. Following injections with hADSCs (1×10^5 cells/body [group DL], 5×10^5 cells/body [group DM], 1×10^6 cells/body [group DH], and 5×10^6 cells/body [group MD]), cardiac function was assessed using an echocardiography system equipped with a 12 MHz transducer (SONOS 7500; Philips, Amsterdam, Netherlands). Heart samples were collected on days 3, 7, 14, and 56 following transplantation.

Two weeks after MI induction, either hADSCs (A group, $n = 20$), hADSCs combined with α GA (final concentration, 10 μ M; A + α GA group, $n = 10$), or α GA alone (final concentration, 10 μ M; α GA group, $n = 4$) were transplanted. For the control group, sham operation was performed (fibrinogen and thrombin solution only; C group, $n = 10$). Cardiac function was examined using echocardiography. Heart samples were collected at days 3, 7, 14, and 56 following transplantation.

Histological analysis of the heart. To assess rCM diameter and fibrosis, heart sections from each group collected 8-weeks after surgery were stained with periodic acid-Schiff and Picro Sirius red, respectively. The sections were also stained with anti-von Willebrand factor antibody, and capillary density was calculated in the peri-infarct area. Electron microscopy was performed for morphological evaluation of mitochondria in the heart.

Quantification of intramyocardial ATP and mitochondrial DNA. ATP content in the heart samples was assessed using a colorimetric ATP assay kit (ab83355; Abcam, Cambridge, UK). To quantify human and rat mitochondrial DNA in the recipient heart, we performed quantitative polymerase chain reaction (PCR). Total DNA was isolated from the infarct region and remote areas, and PCR was performed with SYBR Green (Thermo Fisher Scientific) using specific primer pairs (S1 Table).

Statistical Analysis

All values are expressed as means \pm SEM. Statistical analyses were performed using JMP Pro 14 software (SAS Institute Inc., Cary, NC, USA). Comparison across multiple groups with normal distribution was performed using one-way analysis of variance (ANOVA), followed by Tukey's multiple comparisons test. Comparison between two groups was performed using an unpaired or paired two-tailed Student's *t*-test or Mann-Whitney *U* test, as appropriate. Comparison across multiple groups with non-normal distribution was performed using Kruskal-Wallis tests followed by Dunn's multiple comparisons tests. *P* values < 0.05 were considered statistically significant.

Results

Donor-Derived Mitochondrial DNA Was Detected in CMs In Vivo

Three days after the transplantation of hADSCs harboring pre-stained mitochondria, we detected stained mitochondria in the graft and recipient rat heart (Fig. 2A–D). Electron microscopy revealed tunnel-like connections between hADSCs and CMs (Fig. 2E–G). Laser microdissection was used to obtain heart samples for DNA sequencing (Fig. 2H). The mitochondrial genome fragment was PCR-amplified, and the resulting amplicon length was consistent with those in previous reports (Fig. 2I)¹¹. The genome sequence analysis revealed 99% homology with human mitochondrial NADH-ubiquinone oxidoreductase chain 6 (MT-ND6) (Fig. 2J).

MT Occurred Within 24 h Following Transplantation

For intravital imaging, we transfected hADSCs with CellLight to induce mitochondrial expression of red fluorescent protein (RFP) (Fig. 3A). Upon transplantation, the graft formed a layer on the heart where hADSCs were equally distributed (Fig. 3C). The mitochondria from the hADSCs were detected in the myocardial layer of the recipient, 3–4 h after transplantation (Fig. 3D). Residual CMs in the fibrotic area contained granules that were considered to represent the transferred mitochondria (Fig. 3E, 3F, S1A–C, Video S1, S2). When

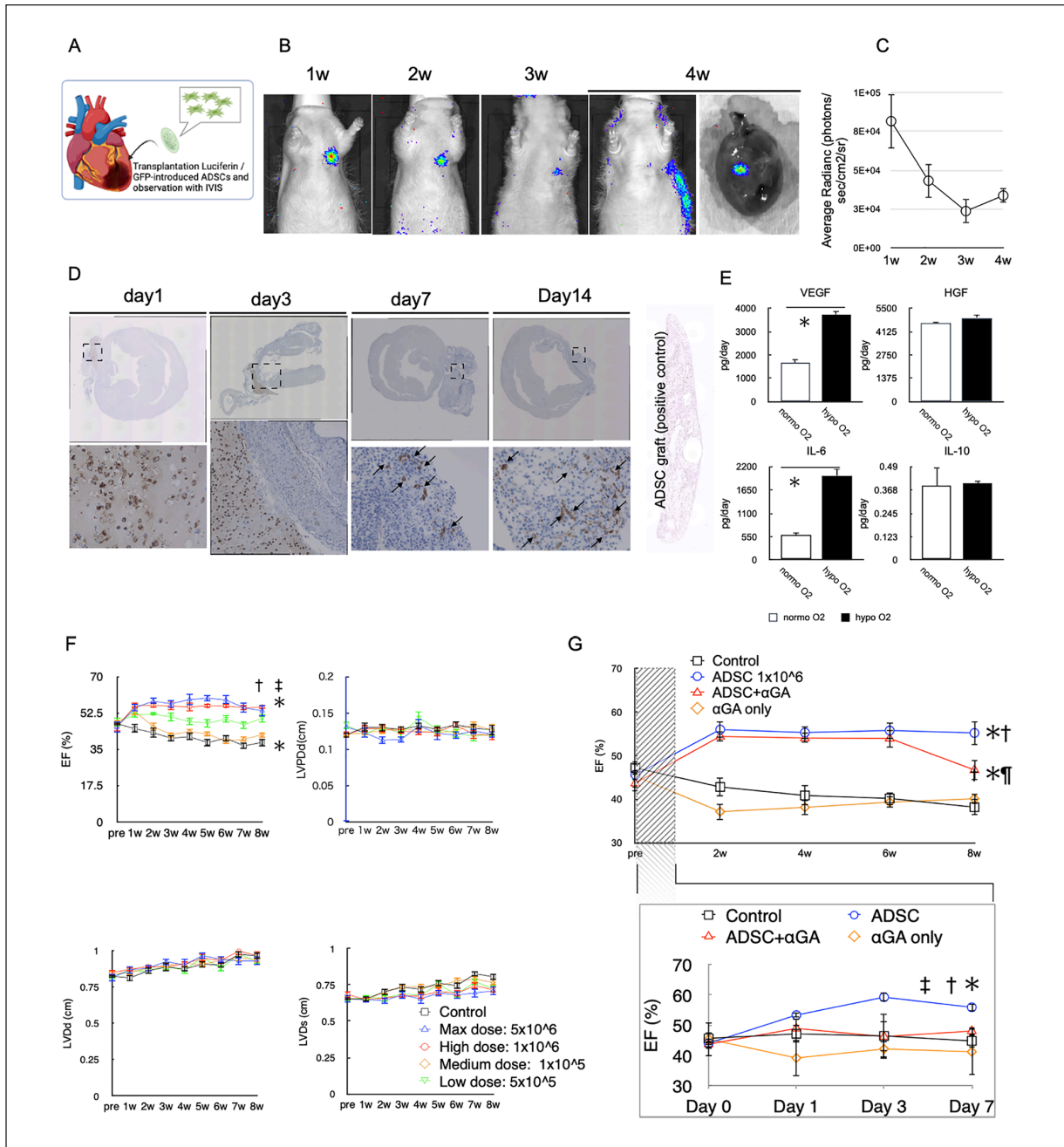


Figure 5. hADSC transplantation into a rat model of ischemic cardiomyopathy. (A) For evaluation of hADSC survival and engraftment, luciferin-transduced hADSCs were implanted on the surface of the heart. (B) Representative images of the luciferin signal from hADSCs. (C) Luciferin signal intensity showing the survival of hADSCs in the graft over time. (D) Representative images of hADSC grafts with stained mitochondria. The lower images are magnifications of the dashed boxes in the upper images. Image on the far right shows the whole graft. It is significant that the survival of the transplanted cells was confirmed not only by tracing the luciferase-transduced hADSC from the body surface but also histologically. (E) Cytokine secretion from hADSC grafts measured by ELISA; $n = 3$ samples per group. * $P < 0.05$ by t -test. (F) Cardiac function and dimension following transplantation; $n = 8$ per group. * $P < 0.05$, † $P < 0.05$, ‡ $P < 0.05$ by ANOVA. (G) Long-term and short-term cardiac function in selected groups after hADSC transplantation; $n = 8$ rats per group. * $P < 0.05$, † $P < 0.05$, ‡ $P < 0.05$, ¶ $P < 0.05$ by ANOVA. hADSC: human adipose-derived stem cell.

co-culture of hADSCs and CMs was performed for 24 h under hypoxic conditions, the hADSCs were found to move around the CMs in a fixed field of view (Fig. 4A, 4B, S2A,

Video S3). In the CMs, the intensity of hADSC-derived mitochondrial luminescence significantly increased during the 24-h co-culture (Fig. 4C). The fixed sample also exhibited

granular hADSC-derived mitochondria in the rat cardiomyocytes (rCM) (Fig. 4D, S2B Video S4).

hADSC Co-Culture Synergistically Enhanced the OCR of CMs In Vitro

The oxygen consumption rate (OCR) of rCMs was synergistically enhanced by hADSC co-culture, and was significantly higher than the sum of the OCRs of rCMs and hADSCs cultured independently. This effect was negated by the addition of a non-specific gap junction inhibitor α GA (Fig. 4E, 4F). We successfully obtained adult rCMs using a Langendorff circuit and captured the motion of individual rCMs (Fig. 4K–M). An additional 24-h culture with supernatant hADSCs had no effect on the contraction of rCMs (Fig. 4N).

hADSC Dose-Dependency and Gap Junction Intervention for Improvement of Cardiac Function

We monitored luciferin signals using an *in vivo* imaging system at least 4 weeks after transplantation. In the fourth week, the heart surface was observed directly (Fig. 5B, 5C). Histological analysis of these samples revealed surviving hADSCs on the surface or in the connective tissue between the heart and chest wall (Fig. 5D). The supernatant of cultured and grafted hADSCs contained various cytokines. Among them, secretion of VEGF and IL-6 was stimulated by hypoxia (Fig. 5E). hADSC transplantation exerted a therapeutic effect on cardiac function in infarcted rats. This effect was temporary in low (DL)- and medium (DM)-dose groups, limited to the early phase following transplantation. In the maximum-dose (MD) group, improvement was greater than in the other groups at weeks 2–6. However, at week 8, cardiac function improved in both the DH and MD groups equally. No effect against cardiac remodeling was observed, as indicated by the left ventricular (LV) end-diastolic diameter (LVDd) and LV posterior wall thickness; however, the LV end-systolic diameter (LVDs) tended to become smaller with increasing doses (Fig. 5F, S1 Fig.). Although the addition of α GA to hADSCs blocked the improvement of cardiac function three days after transplantation, long-term improvement was not affected (Fig. 5G). It was also found that the optimal transplantation time is 1–2 weeks after the onset of MI (S2A–J Fig.).

hADSC Transplantation Increased Intramyocardial Mitochondrial DNA and ATP

No difference was observed in fibrotic area across the groups during the first two weeks following implantation. However, the difference was apparent after 8 weeks. Additionally, semiquantitative assessment revealed less interstitial fibrosis in the hADSC-treated group than in the control group. rCM diameter was significantly smaller in the DH and MD groups,

and the highest capillary densities and lowest collagen accumulation were observed in the DM group (Fig. 6A, B). Mitochondrial number and cristae structure were relatively normal compared to the untreated group, as indicated using electron microscopy. The endoplasmic reticulum, myofibers, Z-disk, and intercalated disks, were confirmed to be morphologically preserved (Fig. 6C). Following treatment, the amount of rat mitochondrial DNA in the myocardium increased with time. However, mitochondrial DNA from the infarct area decreased by day 56 after treatment. In other words, recipient rat mitochondrial DNA increased significantly on day 14 in the infarct area and on day 56 in the remote area (Fig. 6D). Donor-derived mitochondrial genes were not sufficiently amplified to allow detection. One day after transplantation, cytosolic ATP levels in the hADSC-treated group were approximately ten-fold higher than those in the control group (Fig. 6E).

Discussion

Following the transplantation of hADSCs onto the ischemic heart surface, donor-derived mitochondrial DNA was detected in the DNA extracted from CMs, providing the first evidence of MT from ADSCs to the ischemic myocardium *in vivo*. This MT occurred shortly after transplantation, as evidenced by histological evaluation and intravital imaging, suggesting an influence on early improvement of cardiac function. Furthermore, ATP concentration in the intramyocardial infarct area increased 24 h after transplantation and stabilized after a week. Consistent with our findings, previous reports have suggested retention of these mitochondria for approximately 1 week²¹. However, direct histological identification of mitochondria over time was challenging. Although the detailed mechanisms underlying MT nor specific cell type have not been elucidated, our data confirmed cell–cell communication and indicate transfer of mitochondria and other organelles between cells²². Specifically, when CMs were exposed to hADSC supernatant, no immediate contraction-enhancement effect was observed on CMs, suggesting that direct cell–cell communication is necessary for MT to occur between hADSCs and CMs²¹. *In vitro* experiments using a co-culture system demonstrated that ADSCs interact with and transfer mitochondria to CMs, thereby improving their metabolic capacity, as measured by OCR. Moreover, the addition of a connexin blocker to this *in vitro* co-culture system prevented the OCR enhancement effect of MT, and reduced the ability of MT to improve cardiac function *in vivo*, suggesting the involvement of connexin in cell–cell communication underlying MT. However, the survival period of transferred mitochondria, the signaling pathway leading to MT, and the detailed mechanisms of recipient cell activation remain to be elucidated.

Ischemic diseases are often ameliorated by angiogenesis; however, this can lead to the dysfunction of myocardial and cardiac cells. Reactivation of these cells can result in

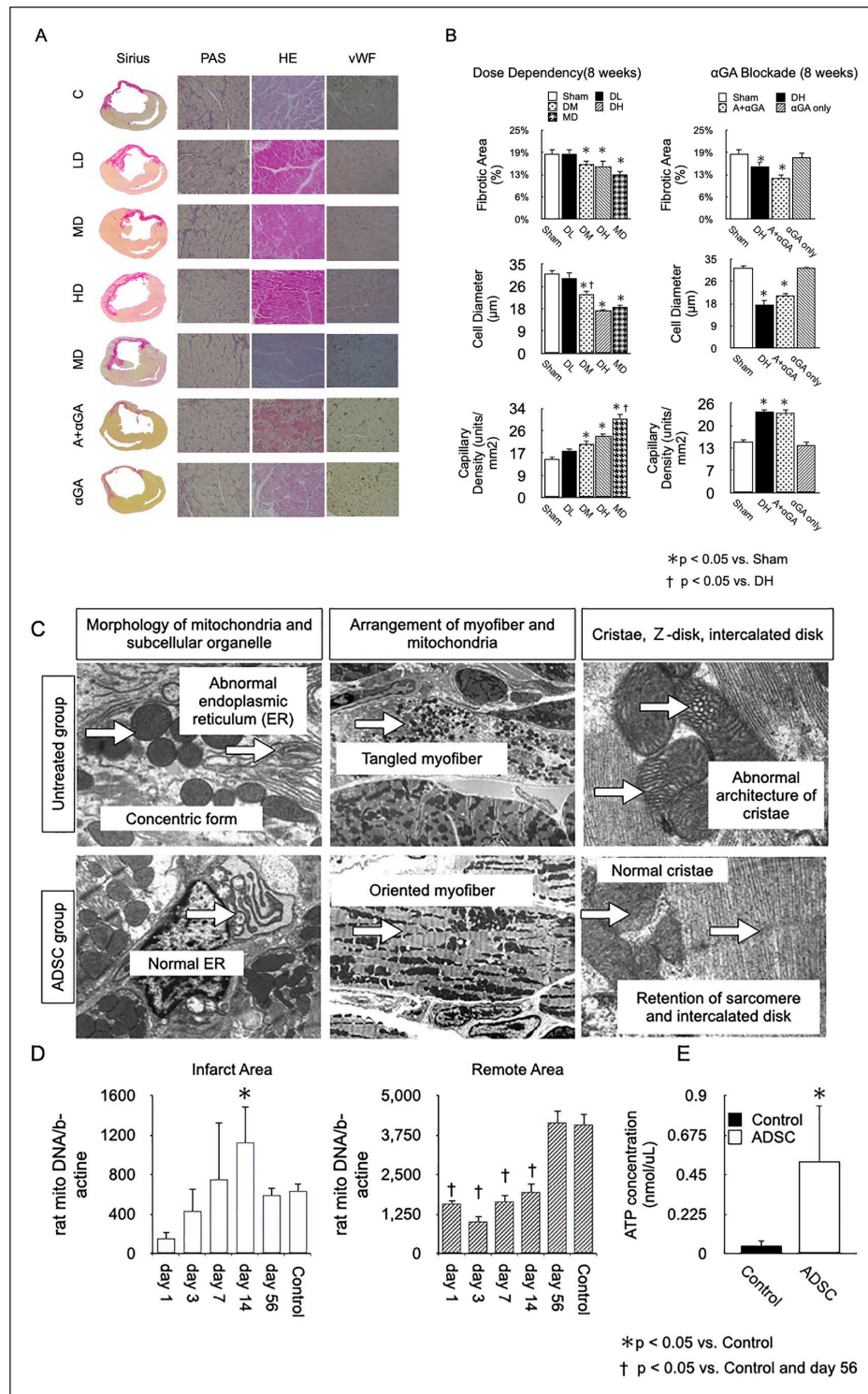


Figure 6. Histological analysis of the heart. (A) Representative whole microscopy images of Sirius red staining, periodic acid-Schiff staining, and immunostaining using an anti-von Willebrand factor antibody in each group; $n = 8-10$ per group, scale bar = $50\ \mu\text{m}$, group DL: 1×10^5 cells/body, group DM: 5×10^5 cells/body, group DH: 1×10^6 cells/body, group MD: 5×10^6 cells/body. (B) Fibrotic area, capillary density, and rCM diameter in each group; $n = 8$ samples for each group; * $P < 0.05$, † $P < 0.05$, ‡ $P < 0.05$, § $P < 0.05$, ¶ $P < 0.05$ by ANOVA. (C) Morphology of mitochondria in rCMs that were observed with an electron microscope after 8 weeks of transplantation. (D) Intramyocardial mitochondrial DNA of the recipient was quantified for each region: infarct and remote areas; $n = 4$ samples for each group. * $P < 0.05$ by ANOVA. (E) Intramyocardial ATP concentration one day after transplantation; $n = 3$ samples per group; * $P < 0.05$ by *t*-test. rCM: rat cardiomyocyte.

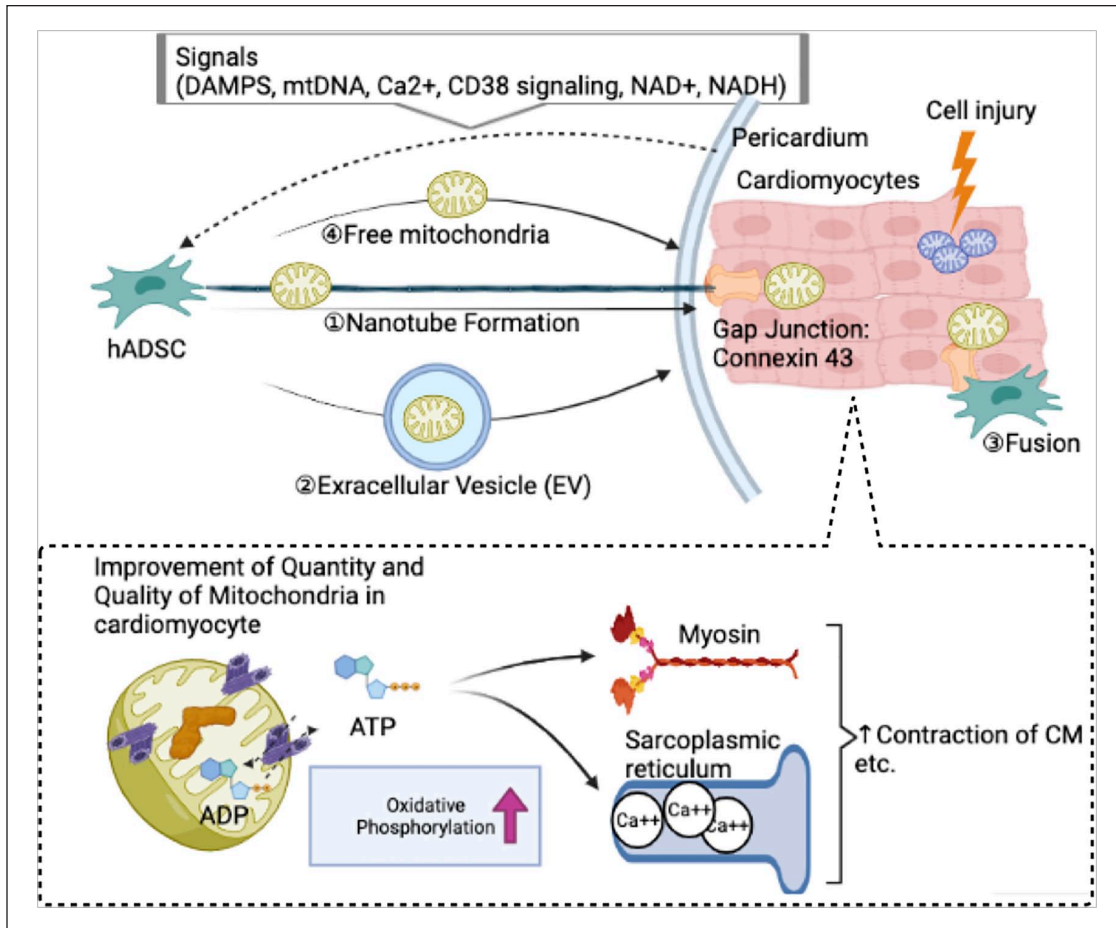


Figure 7. Mode of mitochondrial transfer (MT) and possible mechanism. The possible mechanisms of MT are classified as (1) direct transfer, (2) indirect transfer, (3) fusion, and (4) free mitochondria. Cell injury through hypoxia or free radicals destroys CMs or evokes some form of stress signal. ADSCs receive the signal and transfer their mitochondria to injured cells. Recipient cells enhance their ATP production and contractile power following MT. CM: cardiomyocyte; ADSC: adipose-derived stem cell.

long-term improvement of cardiac function. Although the transplanted cells survived on the surface of the heart for approximately 4 weeks, the transferred mitochondria could not be identified in heart specimens thereafter. Rather, the transferred mitochondria either disappeared within a few days after transplantation, or were present in very low numbers. This suggests that hADSC treatment improves the pathophysiology of ischemic cardiomyopathy, including mitochondrial abnormalities, by providing a short-term supply of relatively healthy mitochondria and normalizing the long-term morphology and quantity of mitochondria in the recipient myocardium.

Mitochondrial protein abnormalities can cause chronic structural abnormalities in heart tissue. Thus, if transferred mitochondria activate pathological mitochondria, it may be beneficial for the subject^{23,24}. Here, structural improvements, such as the orientation of myocardial fibers, suppression of CM hypertrophy, and suppression of fibrosis (remodeling suppression), were observed. These histological changes

could be induced by cytokines from the transplanted cells. Moreover, considering the downward trend of ejection fraction eight weeks after transplantation in the α GA group, MT could be considered to contribute not only to short-term but also long-term improvements in CM function.

Various transfer modes have been proposed for MT, including the involvement of microvesicles, tunneling nanotubes formation, cell fusion, and direct cell-cell contact^{25,26}. It has been reported that connexins are involved in nanotube formation and cell-cell contact among these MT modes. In *in vitro* experiments, danger-associated molecular pattern proteins, mtDNA, Ca^{2+} , CD38 signaling, NAD^+ , and NADH, released from damaged cells, act to trigger signals and actively promote MT from donor cells via the modes shown in Fig. 7²⁷. Additionally, evaluation of the direct myocardial transplantation of isolated mitochondria suggested a mechanism whereby CMs directly internalize mitochondria through the cell membrane²⁸. These processes are considered to be non-specific and reflect passive transfer^{27,29}. Here, MT was

promoted by hypoxic stimulation *in vitro*, and MT from the myocardium to hADSCs was prevented by a connexin blocker *in vivo*. Therefore, ischemic myocardial signaling may be speculated to cause cell–cell communication via gap junctions, after which MT occurs.

In this study, however, the transfer of mitochondrial DNA alone, migration of transplanted cells into the myocardium along with subsequent fusion with recipient cells, and MT via microvesicles could not be excluded. The presence or absence of a signal from the recipient CM to the donor cell (to assess whether MT is active or passive) was not determined, and any potential signal was not specified. Moreover, the amount and period of retention of transferred mitochondria, the mechanisms underlying subsequent increase in intramyocardial ATP, and the short- and long-term improvement of cardiac function remain to be fully elucidated. Nevertheless, our current findings support the hypothesis of cell transplantation delivering living mitochondria directly to myocardial cells, along with cytokines that promote angiogenesis, inducing protective effects in the myocardium⁸. Overall, our results suggested that ADSC-to-CM MT occurs both *in vitro* and *in vivo*, thereby contributing to the recovery of early cardiac function, after ADSC transplantation in ischemic cardiomyopathy. Thus, enhancement of the mechanisms of MT is proposed to enhance the efficacy of cell therapy.

Acknowledgments

The authors are grateful to Dr. Hiroko Iseoka, Dr. Fumiya Oohashi, and Dr. Shohei Yoshida for their invaluable technical assistance.

Ethical Approval

This study was approved by our institutional review board.

Statement of Human and Animal Rights

This article does not contain any studies with human or animal subjects.

Statement of Informed Consent

There are no human subjects in this article and informed consent is not applicable.

Declaration of Conflicting Interests

The author(s) declared no potential conflicts of interest with respect to the research, authorship, and/or publication of this article.

Funding

The author(s) received no financial support for the research, authorship, and/or publication of this article.

ORCID iD

Daisuke Mori  <https://orcid.org/0000-0003-1522-4202>

Supplemental Material

Supplemental material for this article is available online.

References

1. Cahill TJ, Choudhury RP, Riley PR. Heart regeneration and repair after myocardial infarction: translational opportunities for novel therapeutics. *Nat Rev Drug Discov.* 2017;16:699–717.
2. Lopez-Crisosto C, Pennanen C, Vasquez-Trincado C, Morales PE, Bravo-Sagua R, Quest AFG, Chiong M, Lavandero S. Sarcoplasmic reticulum-mitochondria communication in cardiovascular pathophysiology. *Nat Rev Cardiol.* 2017;14(6):342–60.
3. Wu R, Hu X, Wang J. Concise review: optimized strategies for stem cell-based therapy in myocardial repair: clinical translatability and potential limitation. *Stem Cells.* 2018;36(4):482–500.
4. Rustom A, Saffrich R, Markovic I, Walther P, Gerdes HH. Nanotubular highways for intercellular organelle transport. *Science.* 2004;303:1007–1010.
5. Islam MN, Das SR, Emin MT, Wei M, Sun L, Westphalen K, Rowlands DJ, Quadri SK, Bhattacharya S, Bhattacharya J. Mitochondrial transfer from bone-marrow-derived stromal cells to pulmonary alveoli protects against acute lung injury. *Nat Med.* 2012;18:759–53.
6. Brown DA, Perry JB, Allen ME, Sabbah HN, Stauffer BL, Shaikh SR, Cleland JG, Colucci WS, Butler J, Voors AA, Anker SD, et al. Expert consensus document: mitochondrial function as a therapeutic target in heart failure. *Nat Rev Cardiol.* 2017;14(4):238–50.
7. Plotnikov EY, Khryapenkova TG, Vasileva AK, Marey MV, Galkina SI, Isaev NK, Sheval EV, Polyakov VY, Sukhikh GT, Zorov DB. Cell-to-cell cross-talk between mesenchymal stem cells and cardiomyocytes in co-culture. *J Cell Mol Med.* 2008;12(5A):1622–31.
8. Han H, Hu J, Yan Q, Zhu J, Zhu Z, Chen Y, Sun J, Zhang R. Bone marrow-derived mesenchymal stem cells rescue injured H9c2 cells via transferring intact mitochondria through tunneling nanotubes in an *in vitro* simulated ischemia/reperfusion model. *Mol Med Rep.* 2016;13(2):1517–24.
9. Eisner V, Cupo RR, Gao E, Csordás G, Slovinsky WS, Paillard M, Cheng L, Ibeti J, Wayne Chen SR, Kurt Chuprun J, Hoek JB, et al. Mitochondrial fusion dynamics is robust in the heart and depends on calcium oscillations and contractile activity. *Proc Natl Acad Sci U S A.* 2017;114:E859–68.
10. Wang K, Xu Y, Sun Q, Long J, Liu J, Ding J. Mitochondria regulate cardiac contraction through ATP-dependent and independent mechanisms. *Free Radic Res.* 2018;52(11–12):1256–65.
11. Mori D, Miyagawa S, Matsuura R, Sougawa N, Fukushima S, Ueno T, Toda K, Kuratani T, Tomita K, Maeda N, Shimomura I, et al. Pioglitazone strengthen therapeutic effect of adipose-derived regenerative cells against ischemic cardiomyopathy through enhanced expression of adiponectin and modulation of macrophage phenotype. *Cardiovasc Diabetol.* 2019;18:39.
12. Berridge MV, Herst PM, Rowe MR, Schneider R, McConnell MJ. Mitochondrial transfer between cells: methodological constraints in cell culture and animal models. *Anal Biochem.* 2018;552:75–80.

13. Rooney JP, Ryde IT, Sanders LH, Howlett EH, Colton MD, Germ KE, Mayer GD, Timothy Greenamyre J, Meyer JN. PCR based determination of mitochondrial DNA copy number in multiple species. *Methods Mol Biol.* 2015;1241:23–38.
14. Ayala-Torres S, Chen Y, Svoboda T, Rosenblatt J, Van Houten B. Analysis of gene-specific DNA damage and repair using quantitative polymerase chain reaction. *Methods.* 2000;22(2):135–47.
15. Branda RF, Brooks EM, Chen Z, Naud SJ, Nicklas JA. Dietary modulation of mitochondrial DNA deletions and copy number after chemotherapy in rats. *Mutat Res.* 2002;501:29–36.
16. Matsuura R, Miyagawa S, Fukushima S, Goto T, Harada A, Shimozaki Y, Yamaki K, Sanami S, Kikuta J, Ishii M, Sawa Y. Intravital imaging with two-photon microscopy reveals cellular dynamics in the ischemia-reperfused rat heart. *Sci Rep.* 2018;8:15991.
17. Vinegoni C, Aguirre AD, Lee S, Weissleder R. Imaging the beating heart in the mouse using intravital microscopy techniques. *Nat Protoc.* 2015;10(11):1802–19.
18. Hawat G, Benderdour M, Rousseau G, Baroudi G. Connexin 43 mimetic peptide Gap26 confers protection to intact heart against myocardial ischemia injury. *Pflugers Arch.* 2010;460(3):583–92.
19. Li D, Wu J, Bai Y, Zhao X, Liu L. Isolation and culture of adult mouse cardiomyocytes for cell signaling and in vitro cardiac hypertrophy. *J Vis Exp.* 2014;87:51357.
20. Iseoka H, Miyagawa S, Fukushima S, Saito A, Masuda S, Yajima S, Ito E, Sougawa N, Takeda M, Harada A, Lee JK, et al. Pivotal role of non-cardiomyocytes in electromechanical and therapeutic potential of induced pluripotent stem cell-derived engineered cardiac tissue. *Tissue Eng Part A.* 2018;24(3–4):287–300.
21. Kitani T, Kami D, Matoba S, Gojo S. Internalization of isolated functional mitochondria: involvement of macropinocytosis. *J Cell Mol Med.* 2014;18(8):1694–703.
22. Gherghiceanu M, Popescu LM. Cardiac telocytes—their junctions and functional implications. *Cell Tissue Res.* 2012;348(2):265–79.
23. Hallas T, Eisen B, Shemer Y, Ben Jehuda R, Mekies LN, Naor S, Schick R, Eliyahu S, Reiter I, Vlodaysky E, Katz YS, et al. Investigating the cardiac pathology of SCO2-mediated hypertrophic cardiomyopathy using patients induced pluripotent stem cell-derived cardiomyocytes. *J Cell Mol Med.* 2018;22(2):913–25.
24. Joubert M, Manrique A, Cariou B, Prieur X. Diabetes-related cardiomyopathy: the sweet story of glucose overload from epidemiology to cellular pathways. *Diabetes Metab.* 2019;45(3):238–47.
25. Tan AS, Baty JW, Dong LF, Bezawork-Geleta A, Endaya B, Goodwin J, Bajzikova M, Kovarova J, Peterka M, Yan B, Pesdar EA, et al. Mitochondrial genome acquisition restores respiratory function and tumorigenic potential of cancer cells without mitochondrial DNA. *Cell Metab.* 2015;21:81–94.
26. Denuc A, Núñez E, Calvo E, Loureiro M, Miro-Casas E, Guarás A, Vázquez J, Garcia-Dorado D. New protein-protein interactions of mitochondrial connexin 43 in mouse heart. *J Cell Mol Med.* 2016;20(5):794–803.
27. Paliwal S, Chaudhuri R, Agrawal A, Mohanty S. Human tissue-specific MSCs demonstrate differential mitochondria transfer abilities that may determine their regenerative abilities. *Stem Cell Res Ther.* 2018;9:298.
28. Cowan DB, Yao R, Thedsanamoorthy JK, Zurakowski D, Del Nido PJ, McCully JD. Transit and integration of extracellular mitochondria in human heart cells. *Sci Rep.* 2017;7:17450.
29. Wang J, Li H, Yao Y, Zhao T, Chen Y-Y, Shen Y-L, Wang L-L, Zhu Y. Stem cell-derived mitochondria transplantation: a novel strategy and the challenges for the treatment of tissue injury. *Stem Cell Res Ther.* 2018;9:106.